



J6 sailing upwind during testing

Fatigue Prediction Verification of Fiberglass Hulls

Paul H. Miller¹

The growing use of marine composite materials has led to many technical challenges and one is predicting lifetime durability. This analysis step has a large uncertainty due to the lack of data from in-service composite vessels. Analytical models based on classical lamination theory, finite-element analysis, ship motions, probability and wind and wave mechanics were used in this project to predict hull laminate strains, and fatigue tests were used to determine S-N residual stiffness properties of coupons. These predictions and test data were compared against two cored fiberglass sisterships having significantly different fatigue histories and undamaged laminates representing a new vessel. Strains were measured while underway and good correlation was achieved between predictions and measurements. Fatigue damage indicators were identified which could be used in vessel inspection procedures. Endurance limits were found to be near 25% of static failure load, indicating that a fatigue design factor of four is required for infinite service with this material. Standard moisture experiments using boiling water were compared with long-term exposure. Results indicated the boiling water test yielded significantly conservative values and was not a reliable means of predicting long-term effects. Panel tests were compared with a combined coupon and finite-element procedure. Results indicated the proposed procedure was a viable substitute, at least for the materials studied. A rational explanation for using thicker outer skin laminates in marine composites was identified through single-sided moisture flex tests. These showed that the reduced strength and stiffness due to moisture of the outer hull skin laminate could be compensated by increased thickness. Although the resulting unbalanced laminate is not ideal from a warping standpoint, the approach leads to consistent tensile failure of the inner skin when subjected to normal loads. Permeability considerations make this desirable for hull laminates.

Introduction

COMPOSITE MATERIALS are used throughout the marine industry for numerous applications, including hull shells, in-

ternal structure, superstructures, piping, shafts, foundations, ducts, and gratings. Most applications are in recreational and small commercial vessels, with composite use in offshore structures and naval vessels growing rapidly.

The history of composites in the marine environment is about 40 years old. During this time rules-of-thumb have developed that work adequately, if not conservatively, for long-term service. With the development of new materials, however, faster and more reliable methods must be devel-

¹ Department of Naval Architecture & Ocean Engineering, United States Naval Academy, Annapolis, Maryland 21403.

Presented at the April 12, 2001 meeting of the Northern California Section of THE SOCIETY OF NAVAL ARCHITECTS AND MARINE ENGINEERS.

oped to characterize the durability of new composites for marine use. For example, the first 30 years of marine composites were dominated by single-skin construction, but during the last two decades sandwich construction using lightweight cores has found increasingly greater use. This change has required a new, time consuming and expensive learning curve. Durability problems, particularly for below-waterline applications, have surfaced as the new construction process became widespread [1,2]. In addition to safety issues, current empirical methods often do not lead to the most weight-optimized structure [3,4].

Macromechanical stiffness analysis of multi-phase materials is well developed and is based on classical laminated plate theories developed by Timoshenko. They work adequately for most thin laminates [5]. Failure criteria exist for specific multi-phase materials such as wood, concrete, metal matrix composites and polymer based composites, and have greater uncertainty [5-9]. Due to the current marine industry focus, this paper limits its scope to polymer matrix composites using fibrous reinforcements, with common examples including polyester resin and E-glass reinforcement laminates.

This paper addresses the lack of durability data of a common marine fiberglass by correlating current test and analysis methods with full-scale results. The correct use of this method will allow designers to more accurately predict fatigue effects, eliminating the use of somewhat arbitrary factors included in the industry-standard design guides. The research program included the following steps:

1. Review of appropriate materials, laminates, construction and analysis methods representing past, current, and future industry trends.
2. Selection of a representative material and application for verification. Determination of appropriate fatigue loading for the anticipated application through historical review of the vessels' service lives.
3. Verification and modification of current test methods to better reflect actual load conditions, including strain rate, moisture and boundary conditions.
4. Correlation of test methods to numerical analysis and full-scale results.

Current practice

Materials

Typical applications for marine composites include recreational craft ranging from sailboards and canoes to speed-

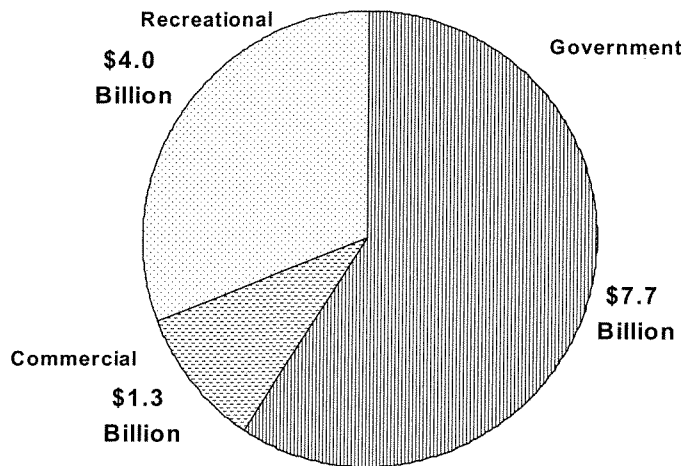


Fig. 1 1993 marine industry segments

boats and motor and sail yachts up to 160 ft [10], military vessels up to 180 ft [11,12], and components of offshore structures [13,14].

Figure 1 shows an estimate of the 1993 marine market expenditure by government, commercial, and recreational segments [15-18]. An important point is that the cost data includes repairs, which skew the results towards the more expensive government and commercial segments as recreational repair data were not available. As roughly 80-90% of recreational craft are made of composites, it is likely that 20-30% of the marine industry used composites in 1993. Trends indicate this is growing.

Typical marine composite laminates consist of reinforcement fibers held in place by a resin matrix system. To increase flexural stiffness and strength in a weight-efficient manner laminates are often made as sandwiches comprising two reinforcement skins with a lightweight core. Numerous resins, fiber and core materials are used. The most common of each type are polyester resins, E-glass fibers and foam or balsa cores [19]. Until the last few years virtually all fabrication was in open molds, and that is still the most common method. Stricter air quality requirements are forcing a change to closed mold fabrication.

Analysis methods

Selected design methods are related to the types of loads encountered and the design complexity. Loads are application-dependent and many are variable and random, and as such, loads typically comprise the largest uncertainty in marine design [20]. Table 1 shows common design loads for marine composite applications [13].

Current design practice is often dictated by the requirements of insurance acceptability or military standards. For the American designer of commercial or recreational craft this often means meeting the requirements of the American Bureau of Shipping (ABS) [21-23].

The marine composites designer is faced with numerous analysis techniques ranging from empirical "rules-of-thumb," to classification society rules and to advanced numerical modeling through finite-element analysis (FEA). The selection of the appropriate method largely depends on the design complexity and owner's requirements. With the increasing power of the personal computer and the wider availability of sophisticated analysis software, more small craft designers are acquiring and applying sophisticated methods [24]. Although many small-craft designers use orthotropic plate

Table 1
Marine loads

Category	Specific Type
Static	combined in-plane loads (buoyancy, cargo)
	large out-of-plane loads (pressures, deflections)
	contact loads (docking, assembly, etc.)
	thermal loads (fire)
Dynamic	shock (>150m/sec) (air and water)
	structural dynamics (slamming, whipping, machinery, rigging)
	wave action, cavitation
	noise, acoustics
Fatigue	low cycle (dives) high cycle (whipping, vibration, waves)
Creep	hydrostatic
Environment	sea water corrosion
	water absorption
	UV exposure fire and smoke

theory, carpet plots, or blended properties to determine laminate mechanical properties, stresses and strains [19,25,26], the most accurate approach uses classical lamination theory (CLT) combined with ASTM tests. CLT relies on Hooke's law, the linear stress-strain relations for an anisotropic material. For typical composite laminates this is simplified by using the plane stress and transversely isotropic assumptions [7].

"Failure" in marine composites relate to a loss of stiffness (generating too large deflections) or strength. Stiffness loss can generally be traced to two phenomena, microcracking and delamination [27]. Microcracking is the generation of small cracks in the matrix which cause discontinuity in load transfer, and delamination is the separation of adjoining plies or the skins from the core. Predicting "loss of stiffness" failure is only accomplished through prototype testing [28]. Strength failures are predicted through failure criteria such as maximum stress, maximum strain, Tsai-Wu [29] or Hashin [30].

Fatigue is the accumulation of stress-induced microcracks that gradually increase in size until large enough to cause fracture. Since fatigue is a cumulative process the onset of failure depends on the magnitude and number of cycles of the various stresses placed on the structure [31]. Two types of "fatigue" are generally encountered in marine composites. The first is dynamic or cyclic fatigue caused by varying loads, for instance, waves or machinery. The other is static fatigue, or creep, from resisting static loads over a long period of time (for instance, a response to the still water bending moment). For most primary structure applications in marine composites, cyclic fatigue causes more damage [32]. Fatigue is a function of both in-plane and out-of-plane load components. As both generally occur in the linear range of material response, these components are usually combined through superposition to determine the stress amplitude range [8].

The basic method to include fatigue effects is to "reduce the material strength properties by a factor of 2 or more" [33]. Although still widely used today [19], this approach is a carry over from metal and wood fatigue tests and the resultant design standards developed over 30 years ago [25]. The assumption used is that the endurance limit (or "fatigue limit") is half of the static ultimate strength [33]. Any stresses encountered below this level would not cause damage accumulation. For composites this is not a good assumption as the endurance limit is driven by the materials and fiber orientation, and can range from over 65% to less than 25% [34]. The endurance limit is important for small craft as one primary stress inducer is wave impact, and many craft may see 10^7 impacts in a lifetime.

Two analytical methods are commonly used for fatigue effects prediction. One is fracture mechanics, which looks at crack growth and the number of cycles for initial defects to propagate to a critical crack length that leads to fracture [31]. This method is gaining widespread use in metals, but is not yet developed enough for woven composite laminates [35,36]. The other method uses empirically-developed S-N curves combined with a damage accumulation model.

The most common damage accumulation model is the linear Miner Rule. In terms of expected damage for a probabilistic stress life:

$$E[D] = T \cdot f \int_0^{\infty} \frac{p(s_i)ds}{N(s_i)}$$

where

$E[D]$ = expected accumulated damage ratio

T = time at frequency f

$p(s_i)$ = probabilistic distribution of number of stress cycles at stress s_i

$N(s_i)$ = number of cycles to failure at stress s_i

Usually failure is assumed to occur when $D = 1$, although for some marine composites tests have shown that failure actually occurs when the accumulated damage ratio is as low as 0.25 [8]. This implies stress sequence history can be significant for composites. This value is different from the limit damage ratio in Ref [31], which is used as a replacement criteria.

Testing methods

As full-scale prototyping is rarely possible, designers rely on data from standardized tests. In-plane tests include ASTM D 3039 (tensile), D 3518 (shear), D 695 and C 364 (compression with and without cores). Out-of-plane fatigue testing is usually performed as a modification of the ASTM static tests for composites (D 790 3- and 4-point flex), or through the use of a specialized composite fatigue test such as ASTM C 393/D 671 [37]. Tests are run at as high a frequency as possible to reduce acquisition time. Dry testing at high frequencies, however, can cause accelerated damage due to heat buildup [28].

Application description

Over a dozen vessel designs were considered for testing verification. The criteria included: availability of sisterships, clear fatigue histories, ability to strain gage the hulls and the ability to accurately model the vessel. Many of the designs were ruled out due to a lack of cooperation by the builders in providing construction details or a lack of documented quality control.

The selection of the J/24 was based on its availability through the strong support of OCSC,² the great support from the builder, TPI, the reduced crew requirements, and its widespread use internationally.

Designed by Rod Johnstone in the mid-1970s, the boat is considered a one-design racer with overnight accommodations for four. Although predominantly used for racing, sailing schools also use the boats for instruction and day charters. The major U.S. builder was TPI, Inc. of Warren, Rhode Island, who built 5186 boats, with the last one in 1995 [38]. Production resumed at a different U.S. builder in late 1999.

TPI donated coupons and panels representing the hull laminate of a new vessel. The construction is polyester resin and E-glass (mostly mat) with balsa core. The inner skin is thinner than the outer skin.

Service histories

J/24 Class Association members assisted in locating a low-mileage and a high-mileage vessel. The two vessels, *Imajination* and *J6*, have seen significantly different service. The procedure for each boat was similar:

- determine how many hours of service the vessel saw,
- correlate those hours to weather data (wind and waves), and
- determine the number of strain cycles and ranges seen.

J6, (the high-mileage vessel) entered the OCSC fleet as a new vessel in December 1984 and began operations in January 1985. Detailed daily records of boat usage were available for January 1996 to June 1999 and were used to develop monthly totals for morning, afternoon and evening use. The data were compared to overall figures from 1985 to 1998, which indicated the annual usage was relatively consistent

² A sailing school in Berkeley, California, that operates boats on the Berkeley Circle, the roughest portion of San Francisco Bay.

Table 2
1998 daily sailing hours for *J6*

1998 Month	Hours Used			total
	AM	PM	Eve/Night	
January	6	16	3	25
February	8	8		16
March	10	28		38
April	32	57	4	93
May	26	48	3	77
June	28	34	5	67
July	31	49	4	84
August	32	39	2	73
September	26	46	6	78
October	32	41		73
November	24	42	3	69
December	8	12		20
Totals	263	420	30	713

from year to year. Table 2 shows the amount of usage per daily time period and month for 1998, and is typical of those from 1996–1999. “AM” hours are 9 AM to 1 PM and “PM” hours are 1–5. “Evening/Night” hours are after 5 PM. Typical usage included sailing lessons, charters by members and the occasional special event. Only those hours spent underway outside the breakwater were included due to the calm conditions inside the harbor. Figure 2 shows the month-to-month usage of *J6* from 1996 to 1999. The total predicted hours sailed since new is 11 300 with a coefficient of variation (COV) of 12%.

The first “low-mileage” vessel tested was built in 1995. This vessel had been in a substantial collision, however, and was found to be less stiff than *J6*. Another low-mileage vessel was located. *Imagination* was built in 1981 and entered OCSC service in 1999. Her owner from 1993–1999 indicated she had been lightly used on a lake most of her life, and she had strong indications of little use. Using data from *J/Boats* market research of average owner’s use, she was estimated to have seen approximately 740 hr of use, with a COV of 20%.

Wind data were supplied by WindCall [39] which has a recording anemometer located approximately one-half mile

downwind of the primary sailing location. Winds below 10 knots were not recorded; however, this was not a problem as later analysis indicated the fatigue endurance limit was limited to conditions where the wind exceeded 13 knots.

The daily data files included time, lull wind speed, gust wind speed, and 15-min average wind speed. As the boat records indicated *J6* only rarely sailed after dark (<2%), the data were filtered to include only those wind readings taken between 9 AM and sunset. These data were then used to predict significant wave height, rig tension, boat speed and eventually local hull strains through finite-element analysis.

Studies at U.C. Berkeley in the 1970s [40] showed the JONSWOP wave spectrum best approximates that found in the central portion of San Francisco Bay. This spectrum was developed for the shallow North Sea where the fetch is limited but deep water waves can develop [41]. Although this spectrum does a good job for the deeper portion of the Bay (where the earlier study was located), the depth in the Berkeley Circle averages near 10 ft, which gives a typical wavelength to water depth ratio of 2.4. This implies the wave dynamics follow an “intermediate-wave pattern” [42]. The U.S. Army Corps of Engineers extended the JONSWOP spectrum for intermediate and shallow water effects [43], and their formulas were used to predict wave height and period.

The number of stress cycles is primarily a function of wave encounter frequency, which is based on a ship’s speed and course, and the time underway. To predict the *J/24*’s speed under sail for a given wind strength the IMS velocity prediction program was used [44]. The results and the input headings were modified by taking course and GPS data during actual sailing lessons. From these the course distribution for typical lessons is shown in Table 3.

The wind speed, wave period, boat speed and heading distributions were applied to the boats’ hourly usage, resulting in predictions of 10.2 million wave encounters for *J6* and 600 000 encounters for *Imagination*. Encounter frequencies ranged from 0 to 0.71 Hz.

Testing

The testing program included coupon, panel and full-scale tests.

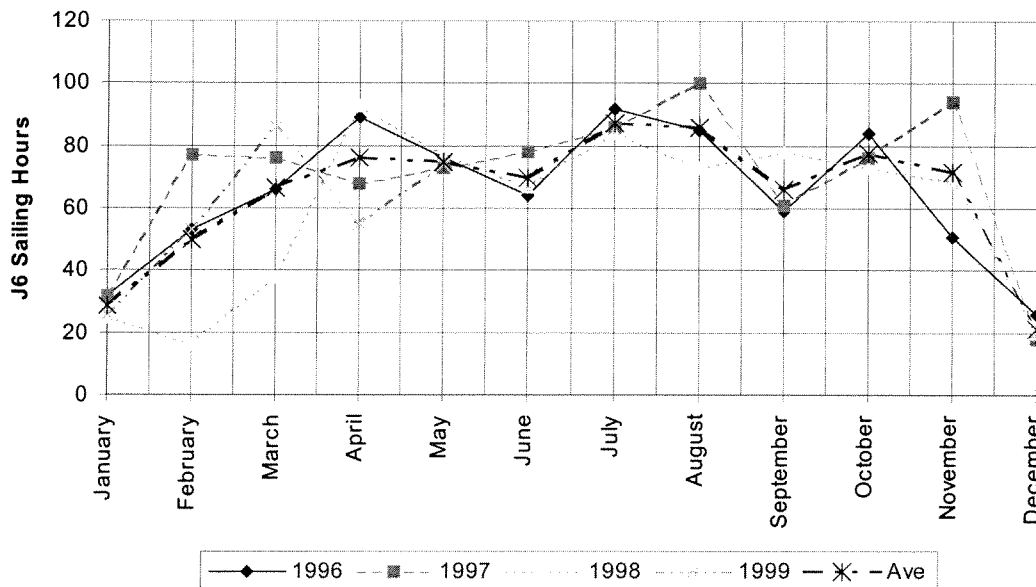


Fig. 2 Month-to-month usage of *J6* from Jan. 1996 to June 1999

Table 3
Course distribution

Beating (true wind angle=45 deg)	60%
Reaching (true wind angle=90 deg)	25%
Broad Reaching (true wind angle=135 deg)	15%

Coupon testing program

The material testing program's goals were to:

- Compare environmental testing approaches.
- Determine the material properties needed for the finite element analysis.
- Compare coupon and panel test methods to full-scale results.

Environmental testing included submerged, relative humidity and boiled conditions. Mechanical testing included:

- tensile (ASTM D 3039), 21 specimens
- compressive (seven with core: ASTM C 364)
- compressive (21 without core: ASTM (Boeing Modified D 695)
- shear (ASTM D 3518), 21 specimens
- flexural fatigue (ASTM C 393/D 90), 50 specimens

Environmental testing—Small craft can be either “wet” or “dry” stored, depending on whether they are kept in the water permanently or just put in for the activity. To accurately model boats remaining in the water, test results providing weight gain and property effects caused by immersion were necessary. These tests also allowed for comparison of standard industry approaches for determining moisture effects.

The basic process through which moisture is absorbed into a polymer composite laminate can be described by Fickian diffusion. For a typical polyester/E-glass marine-type laminate, the constants are close to $M_{\text{initial}} = 0.05\%$, $M_{\text{max}} = 1.8\%$, $D_x = 7 \times 10^{-7} \text{ mm}^2\text{s}^{-1}$ [45], where M refers to the initial and maximum moisture content and D_x is the diffusion constant. Variations of 200% are relatively common for D_x , and M_m appears sensitive to temperature, with increases of 2–5 times for temperature increases of 10–50°C [45].

To determine the moisture absorption, six specimen sets consisting of two groups of three sets, (ASTM tensile, shear and compression specimen sets, all without cores) were exposed to moisture. One group was submerged in tap water and the other group was exposed to 100% relative humidity. Both were kept at room temperature. Each set had seven individual coupons. The moisture specimens were placed in the steam saturation room in 460 Davis Hall at the University of California at Berkeley in early March 1998. A third group was kept dry.

The specimens were regularly weighed and measured. After 226 days the specimens exposed to the relative humidity had gained an average of 1.32% weight, while the submerged specimens gained 1.72%. The coefficient of moisture expansion was 0.023%. The best-fit to Fickian diffusion gave $M_i = 0.07\%$, $M_m = 1.72\%$, $D_x = 5 \times 10^{-7}$.

To see the effect of sealing the edges on weight gain the relative humidity specimens were removed from the steam room and allowed to dry. After one month the weight had stabilized to the dry coupon weight and the edges were then lightly sanded and coated with epoxy. The sealed edge specimens were then submerged with the other specimens. After weighing on the same schedule as the original unsealed specimens, the moisture absorption was found to be identical to the unsealed submerged specimens, indicating the edges were not a significant moisture absorption path in these uncured laminates.

Tests were also performed to determine the effect of different moisture tests on strength. One batch of specimens was kept dry at room temperature. Another was kept submerged in tap water at room temperature for 15 months. The third batch was kept at 100% relative humidity for 15 months and then boiled for 24 hr. The boiling approach simulates a common method for accelerated aging.

The boiling water specimens showed different tensile strength and physical properties from the long-term submerged specimens. After boiling, the specimens were uniformly a lighter shade of green, indicating some change in their physical characteristics. In addition to the lower tensile strengths than the wet specimens, the boiled specimens also exhibited lower levels of audio response. Whereas the dry and wet specimens typically reached a point of 5500–6000 psi before continuous “pinging” was heard, the boiled specimens reached this level at 4000–5000 psi. This could be a sign of greater brittleness in the resin causing early microcracking. It appeared that using the boiling water test applied an extra level of conservatism in the physical properties.

Tensile test results—Twenty-one test specimens were tested for tensile strength and modulus using ASTM D 3039. The specimen dimensions were 1 in. wide by 10 in. long (approximately 0.15 in. thick) and were tabbed with two layers of DB170 (17 oz/yd² ± 45° E-glass fabric) on each side within 1 in. of the ends. Three of 21 specimens broke in the grips. Fifty percent of the specimens broke in the middle and the remaining within 1 in. of the tabbing. Table 4 shows the results.

Shear tests—Twenty-one test specimens were tested for shear strength and modulus using ASTM D 3518. The specimens were the same as the D 3039 specimens with the exception that the cloth layer was laminated at 45° to the pull axis. Table 5 shows the results.

Compression tests—Twenty-one uncured and seven cored compressive specimens were tested using the ASTM (Boeing Modified) D 695 (without core) and ASTM C 364 (with core) test standards. The uncured specimens were subjected to the same environmental conditions as the tensile and shear specimens. The cored specimens were tested dry. Modulus was measured by the crosshead movement and checked with strain gages.

The difference in the two test standards relates to the likelihood of buckling as a failure mode. In the case of the sandwich laminates the core helps stabilize the specimens. To compare the two methods the uncured specimen values were compared to the failure stress of the cored specimens with an allowance for the core removed, making the assumption that apart from buckling resistance, the core provided negligible compressive strength. The cored specimens had a normalized compressive strength 20% less than the uncured. Table 6 presents the uncured compressive test results.

Again the wet specimens showed a significant drop in properties. Of interest is the difference between the tensile and compressive strength values, with the compressive strength more than twice that of the tensile values. This is probably due to the very low fiber volume (~25%) in the laminate, making the laminate act more like a resin than a glass composite.

Table 4
Tensile tests results

Exposure	Ave Tens Str.	% dif	Ave Tens Mod.	% dif
	ksi		msi	
Dry	11.3		1.19	
Wet	9.4	-20%	1.05	-12%
100% RH/24 hr boil	8.6	-24%	1.03	-13%

Table 5
Shear tests results

Exposure	Ave Tens Str	% dif	Ave Tens Mod	% dif
	ksi		msi	
Dry	11.3		1.19	
Wet	9.4	-20%	1.05	-12%
100% RH/24 hr boil	8.6	-24%	1.03	-13%

Table 6
Compressive test results

Exposure	Ave Comp Str	% dif	Ave Comp Mod	% dif
	ksi		msi	
Dry	25.3		0.92	
Wet	21.2	-16%	0.86	-6%
100% RH/24 hr boil	18.9	-25%	0.80	-12%

Static flexural coupon testing—Static flexural testing was performed to determine the out-of-plane properties, validate the FEA, compare test methods and create a baseline for the flexural fatigue tests. These tests are important as out-of-plane loading is the significant loading for small craft [33], and flex tests are often used to qualify small craft laminates [19]. Flex testing included both 3- and 4-point tests based on the commonly used ASTM C 393 (sandwich) and D 790 (uncored) standards.

The first tests included 3- and 4-point ASTM C 393 tests to determine the test effects on predicted properties and select the method for the fatigue testing. The COV for the 3-point tests was 13% and for the 4-point tests was 4.2%. Because of this and the greater ease of strain gaging, the 4-point jig was used for subsequent tests.

When the specimen length changes, the ratio of core shear loading to face sheet loading also varies. In general, the longer the span, the higher the bending moment and the higher the skin stresses. This better approximates the in-service conditions where the supports are the bulkheads and frames. In the 3-point testing the 12 in. specimen tested using ASTM C 393 resulted in a suggested 8 in. span and 16:1 span-to-depth ratio. The 4-point tests were initially set with quarter-point spacing and a 14 in. span. In the test batch one specimen broke by core shear, so the span was increased to 16 in. All subsequent failures were on the tensile face due to the thinner inside skin laminate. Figure 3 shows the 4-point test jig with a specimen.

Comparing the results to the tensile tests gives an indication of the grip effects. The predicted tensile face failure strains in bending were 0.95%, compared to 0.93% for the tensile tests.

As the vessels live in the water a comparison of wet and dry material properties was required. This meant that the outer

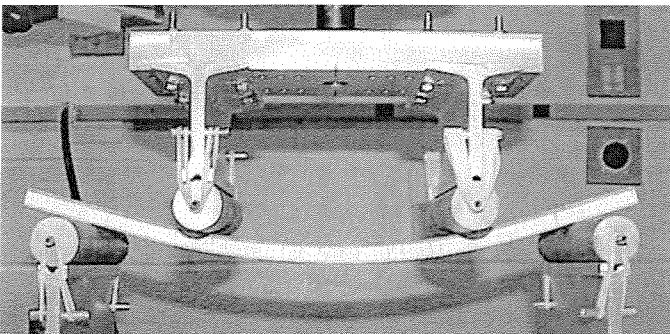


Fig. 3 Four-point flex jig

hull laminate needed to reach submerged moisture equilibrium while the inner skin reached equilibrium based on a high relative humidity. To accomplish this the specimens were soaked in a pool of water equal to the thickness of the outer skin. To avoid moisture absorption into the balsa core the exposed balsa was coated with lacquer and varnish. This provided a waterproof yet flexible coating that would not increase the specimen stiffness or strength. After two months of soaking, mildew was present on the specimen edges, but no discoloration or soaking of the balsa was observed. Using a 16 in. span, 4-point jig, the dry specimens' static ultimate strength was 11 000 psi versus 10 800 psi for the single-sided wet specimens, a decrease of 1.8%. The COV for both sets was 18%. The flexural modulus was the same for both at 1.16 msi (10⁶ psi), with a COV of 8% for the dry and 1% for the wet specimens.

It is interesting to note that the failure of the wet specimens was not significantly lower than that of the dry specimens. Although previous tests showed that all material properties decreased as a result of submergence, for this laminate where the outer skin was substantially thicker than the inside laminate the primary failure mode of both the dry and wet specimens was tensile failure of the (dry) inner skin.

Flexural fatigue testing—A 4-point test jig was designed to cycle up to 50 specimens at one time. Each batch of 10 was deflected to a percentage of the maximum static deflection corresponding to stress ranges of 12.5%, 25%, 37.5%, 50% and 75% of dry static strength. Results from these tests yielded a stiffness-based S-N curve. The drive motor was a Baldor 5 HP, 3-phase "SmartMotor," which included a built-in controller. In-service modifications included removing the cams for the 75% and 50% load cases. This was done and due to the relatively low number of cycles-to-failure these specimens were more efficiently tested on the Satec 50UD machine.

The wet specimens were tested out of the water, although they were run for a maximum of 6 hr each day. The remaining time was spent soaking. Given the low moisture diffusion rate, this was not expected to cause a significant deviation from a fully submerged condition. Indeed, on more than one occasion visible moisture was still apparent on the compression (upper) surface after 6 hr of testing.

One decision concerned the frequency of loading. Too high a loading rate would cause the specimens to generate high internal heat, which would reduce the predicted strength as the temperature approached the heat distortion temperature. Numerous researchers have looked at this problem and have determined the upper bound as 10 Hz for similar materials [6,34,46]. One difference from their tests was that their materials were not cored. As the core would provide insulation, the risk of heat build-up was present.

The "ideal" situation would be to test the materials at the maximum wave encounter frequency [32], which for a J/24 on Berkeley Circle was 0.71 Hz. This would duplicate as close as possible the actual loading conditions, but would significantly increase testing time. The practical solution was to use a thermocouple to measure the temperature. The frequency was increased until the surface temperature at the loading points increased slightly over room temperature. The maximum frequency was 5 Hz for the lowest loaded specimens and 0.5 Hz for the specimens cycled at 75% of the static load. Although the low-cycle load frequency was lower than that in the field, this was not a concern as the heat build-up in the field was considered negligible due to normal cooling from the water and the short duration.

To relate the stiffness measured in the J/24 to the samples, the residual stiffness was calculated after a given number of cycles at the various stress levels. The stiffness measurements used a force control limit of 30 pounds, which equaled

the 12.5% loading level. Figure 4 shows the effect of multiple cycles of the hull laminate. In the plot the stiffness is normalized to the single-cycle dry stiffness at that percent load stress. The COV for all the measured stiffness of a given test group ranged from 2% to 6%. In Fig. 4 the wet and dry specimens of each load have the same color and marker type, with the wet specimens having dashed lines and hollow markers.

The results indicate some general trends. First is the influence of moisture on the outer skin. All the single-sided moisture exposure specimens had lower initial and final stiffness values than the comparable dry specimens. This was due to the reduced stiffness values on the moist side. The loss of stiffness, however, was not significantly different between the wet and dry specimens. This was likely caused by the consistent tensile failure of the inside skin. This was due to the lower tensile versus compressive strength and location of the neutral axis nearer the thicker outer skin.

The progression to failure included an initial audio response combined with whitening under the cloth layer (the outer layer of the inside skin was cloth, the inside layers were mat), followed by whitening of the cloth layer. Failure tended to occur when the flexural stiffness dropped about 25% from its initial value. In some cases (most notably the 50% dry specimens), the stiffness stabilized while crack size propagated.

Failure initiation occurred randomly throughout the constant moment section, and no influence of edge effects or load points was seen.

Panel testing

The panel testing program's goal was to compare FEA predictions based on coupon tests with actual panels. This had two intentions. First, it would give a good indication of the FEA's accuracy to predict full-size vessel responses and indicate whether linear or nonlinear analysis would be required for sufficient accuracy. The secondary goal was to determine if FEA combined with coupon test results could be a viable substitute for panel test methods.

Testing included pressure loading a panel that had moisture conditions representing a boat that is either wet or dry sailed. This had the inner skin dry (80–100% relative humidity) and the outer skin either wet or dry. As with the flexural specimens the balsa edges were sealed with lacquer and varnish to prevent moisture entering the core or inner skin and the panels were soaked for at least two weeks in 0.1 in. deep water (the outer skin thickness is 0.095 in.). The boundary

conditions were simply-supported around the perimeter. To allow the specimen to overhang the edges the restraining jig was made 23 in. square.

A normal pressure load was applied from 0 to 15 psi and string pots measured the panel center point and frame deflections. A strain gage also measured the center strain. The jig was clamped to a rigid steel base with a pressure bag placed between the base and the panel and the panel lying between the bag and the jig. Figure 5 shows the panel jig and Fig. 6 shows the strain and deflection plots. In Fig. 6 the deflection curves are the upper plots.

Full-scale testing

Underway testing included sailing the vessels upwind (close-hauled) and downwind (broad reaching) in San Francisco Bay on both tacks and recording the data. The course took the boats from Buoy F (leeward) to Buoy G (windward) in the Berkeley Circle. This placed the testing directly upwind of the Point Isabel WindCall station and at the northern edge of the Berkeley Circle. The same helmsman, sail trimmers and crew were used for both boats, minimizing the variation in sailing techniques. On each leg the crew positioned themselves in the same location to minimize differences in righting moment. The frontispiece shows *J6* sailing upwind during testing.

After the first boat recorded about 20 min of data, the acquisition system, crew and sails were moved to the other boat and testing repeated. This ensured the testing was completed in as near identical conditions as possible. The first data set was taken between 1:15 and 2:30 PM. The second was taken between 3:30 and 4:30. Figure 7 shows the Pt. Isabel WindCall plot for July 20 [39]. The plot shows similar average winds during the two test periods although the gust peaks were higher at the end of the first period. The higher average wind speed between the test periods may have caused an increase in wave height. Photos of the testing, however, did not indicate a change in wave height.

Data were acquired on a laptop and included vertical accelerations at Station 3.5 and strain gage data from six locations (four hull and two rig). Figure 8 shows the strain on the inside hull laminate (on and off centerline, the upper data are the off-centerline plot on the leeward side). The peak strain was 0.136% for an average wind speed of 14 knots. In both plots the peak period closely corresponds to the predicted wave encounter period.

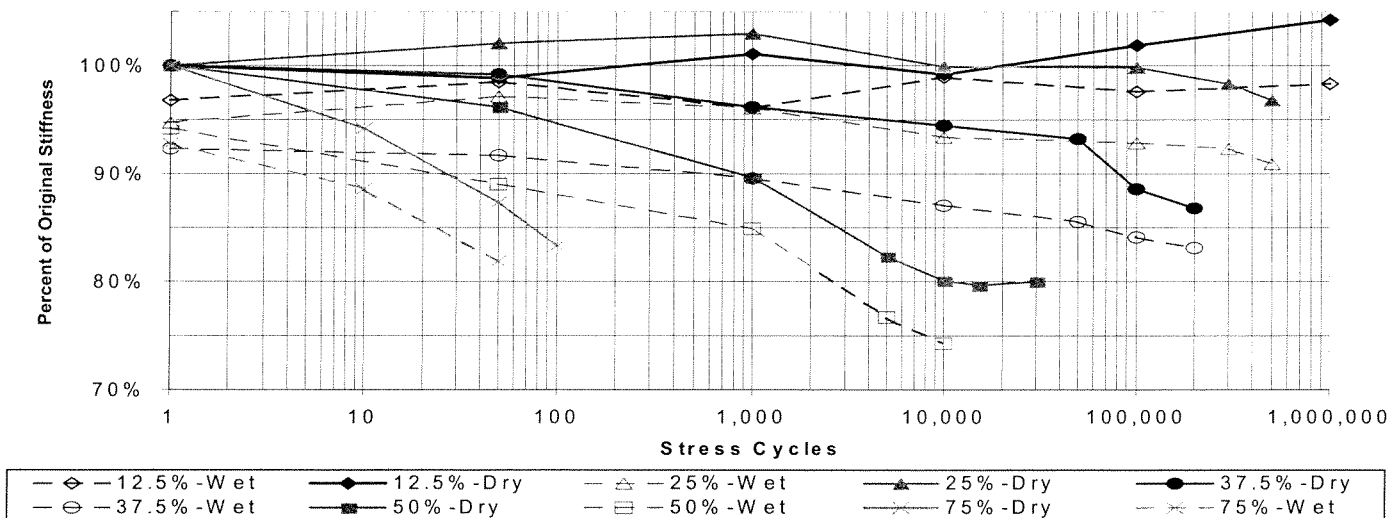


Fig. 4 Stiffness S-N curves for J/24 hull laminate

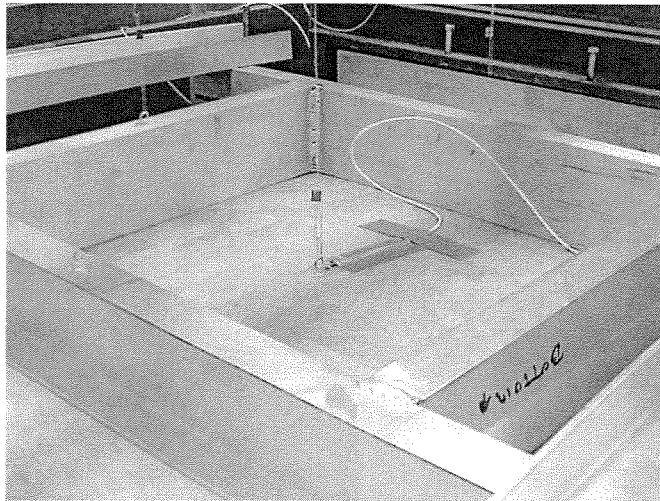


Fig. 5 Panel jig showing strain gage and string pots (10 psi)

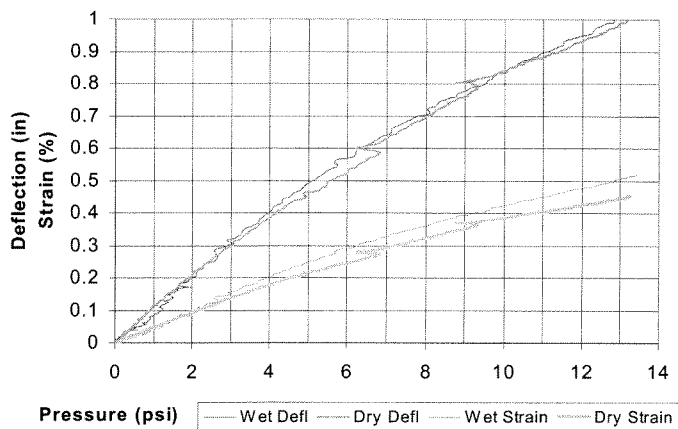


Fig. 6 Load vs. deflection and strain for panel test

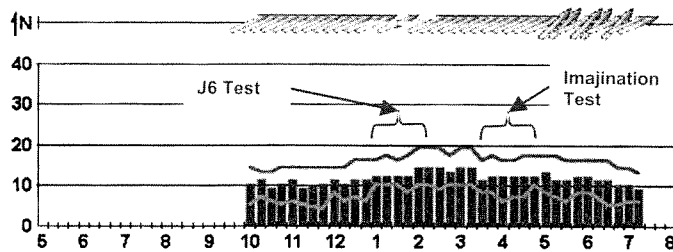


Fig. 7 Wind data from full-scale testing

Correlation with numerical models

Finite-element analysis (FEA) has rapidly grown in its use as a design tool for marine applications where structural complexity and a requirement for accuracy precludes the efficient use of closed-form solutions. The goal of using FEA in this project was to validate its use when correlating between coupon and panel tests and actual vessel performance. This confidence would then allow for FEA strain prediction to be used in fatigue analysis of composite vessels.

The greater potential accuracy of FEA over other design methods can drastically reduce the level of uncertainty when used properly. Designers must always remember the limitations of FEA, however, and avoid problems such as those cited in Sleipner A [47]. For example, composite vessel global

FEA does not accurately model joints and the designer must analyze these separately or include adequate factors of safety. The commonly used plane stress elements also are limited to in-plane stress results, ignoring dominant failure modes in core materials. In all cases it must be remembered that FEA assumes a material continuity in both geometry and material properties. "Low-tech" composite materials have large enough manufacturing variances that this assumption is often suspect. Property COV's of 10% are common in many low-tech laminates [8,19,25,48].

Due to the complexity of the structural system, FEA was used extensively in this project to correlate and predict strains. This included coupon, panel and full-scale vessel analysis. The primary FEA code was an off-the-shelf code (COSMOS/M) and was verified using standard element robustness and accuracy checks [49]. In addition to the Tsai-Wu criteria [29] included in COSMOS/M, post-processing using the Hashin failure criteria [5] and the fatigue analysis were performed using spreadsheets.

The software was limited to three element types for composite analysis: linear plane stress, nonlinear plane stress and solid. All use CLT as the basis for their element stiffness calculation and the determination of directional stresses and strains. The plane stress elements are based on Mindlin shear deformation theory [50]. The difference between the two plane stress elements is that the nonlinear element allows for nonlinear in-plane shear deformations. The solid element allows for linear out-of-plane shear deformations. The analysis itself could be either linear or nonlinear, with the nonlinear effects of large deformation and modulus included.

The material properties derived from the coupon tests described previously, and shown in Table 7 were used as inputs to the FEA.

Coupon FEA

The tensile, shear and compressive models used 2-D laminated shell elements. In general the FEA predictions for stiffness and strength were within 5% of the measured values, with the exception of the tensile specimen model which underpredicted the strength by 13%. This was likely due to the grip effects which caused a stress concentration at the edge. This lowered the average strength values used in the FEA.

The flexural models mainly compared the different element formulations. Initial results indicated the FEA significantly underpredicted both the deflections and the strength. One cause was the boundary conditions which were initially modeled as fixed on one support and pinned (free to slide laterally) at the other. When the sliding pin had friction effects added (the measured coefficient of friction between the steel rod and the boat cloth surface was 0.43) the stiffness accuracy increased to within 3%. The strength issue was largely due to the inherent uncertainty in the tensile testing which provided the material property input to the flexural FEA.

Another reason for the strength discrepancy is the way the FEA shell elements are formulated in COSMOS/M. Linear shell elements tend to underestimate membrane stresses when the deflections are greater than the thickness of the laminate, leading to larger predicted deformations [49]. Additionally, although the elements include bending and some membrane stresses (through an in-plane stiffness addition term), the linear shell elements used in COSMOS/M are based on Mindlin rather than DiScuiva [51] formulations that better account for the core contribution. Regardless, the final difference of 6% for the linear analysis and 4% for the nonlinear analysis with the shell elements is sufficient for

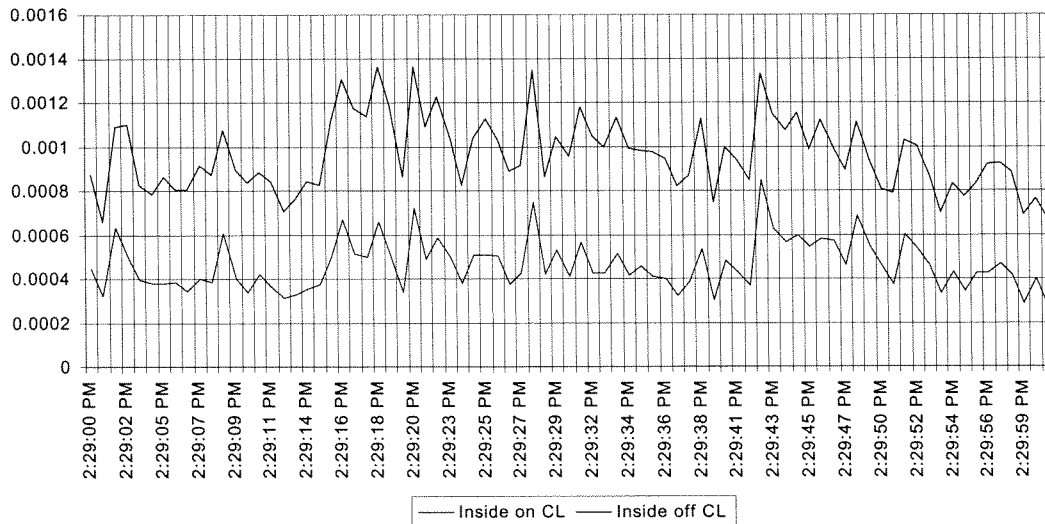


Fig. 8 Inside hull laminate strain gage data from underway testing of J6

Table 7
Final material properties for J/24 FEA

Material	Gelcoat	1.5oz Mat	2,415	Balsa	10oz Boat	24oz Woven	Plywood	Aluminum	Paint	
FEA MPROP#	1	2	Fabmat	Core	Cloth	Roving	6	7	8	9
Ex, Ey [psi]	490,000	920,000	1,400,000	25,000	2,450,000	2,450,000	945,000	10,000,000	100,000	
Ez [psi]	490,000	490,000	490,000	370,000	490,000	490,000	47,000	10,000,000	100,000	
nuxy	0.300	0.361	0.108	0.300	0.067	0.070	0.050	0.330	0.300	
Gxy [psi]	245,000	437,500	700,000	10,000	700,000	700,000	400,000	3,800,000	50,000	
Gxz, Gyz [psi]	245,000	437,500	700,000	18,000	700,000	700,000	400,000	3,800,000	50,000	
Xt, Yt [psi]	11,000	9,427	30,300	1,320	49,000	45,000	6,000	35,000	10,000	
Xc, Yc [psi]	18,000	21,238	24,000	1,187	43,000	40,000	6,000	35,000	5,000	
XYt [psi]	6,000	4,928	14,000	315	14,000	14,000	250	15,000	2,000	
Ply thickness [in]	0.012	0.047	0.073	0.365	0.013	0.038	0.500		0.050	
Density [lb/in ³]	0.0400	0.0570	0.0590	0.0048	0.0610	0.0610	0.0185	0.0966	0.0400	
Density [mass]	1.04E-04	1.48E-04	1.53E-04	1.24E-05	1.58E-04	1.58E-04	4.79E-05	2.50E-04	1.04E-04	
Failure Strain	2.2%	1.0%	2.2%	5.3%	2.0%	1.8%	0.6%	0.4%	10.0%	

most engineering applications as long as it is included in the reliability analysis.

Panel FEA

Panel finite-element analysis was performed with two goals in mind. The first was to determine the mesh density needed in the global model, and the other was to correlate the panel tests to the FEA results. This test program also served as a "bridge" of test results between the coupon and full-size testing.

The mesh verification consisted of refining the mesh until the panel deflections were within 1% of the closed form solutions. This occurred when 10 elements were used between supports.

Initial panel linear FEA matched the measured panel deflections up to 25% of the failure strain. Although potentially sufficient for modeling high-cycle fatigue, greater accuracy was desired. Nonlinear geometric analysis increased the accuracy to about 50% of the failure strain. As the stiffness was over-predicted but the curve's shape was correct, the feeling was that the deflections in the aluminum frame might be causing the error. Figure 9 shows a typical displacement plot of the FEA model with the frame. The panel and frame elements were connected through coupling equations that al-

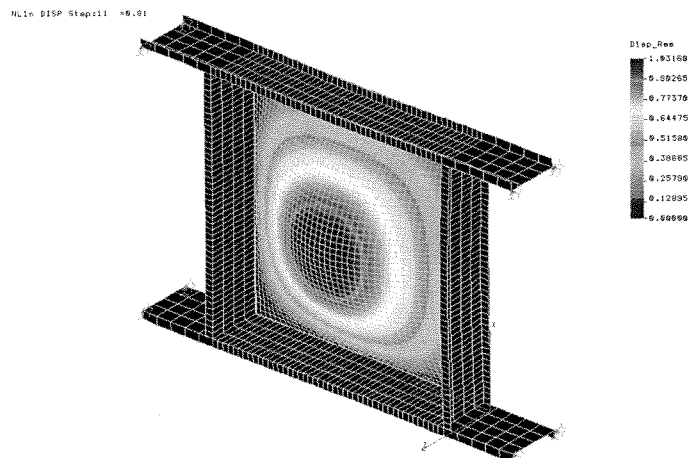


Fig. 9 Displacement plot of FEA panel model

lowed for relative rotations but no translations by the panel into the frame. This duplicated the simply-supported boundary conditions in the original panel models.

Figure 10 shows the predicted and measured displacements and Fig. 11 shows the measured and predicted strains

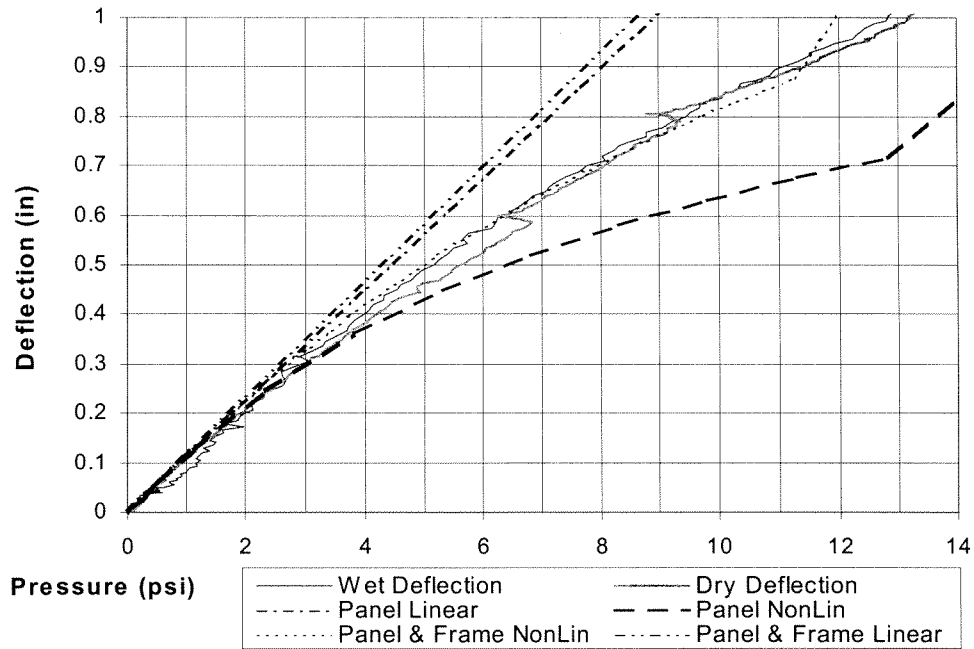


Fig. 10 Load-deflection curves for pressure loaded J/24 hull panel vs. FEA predictions

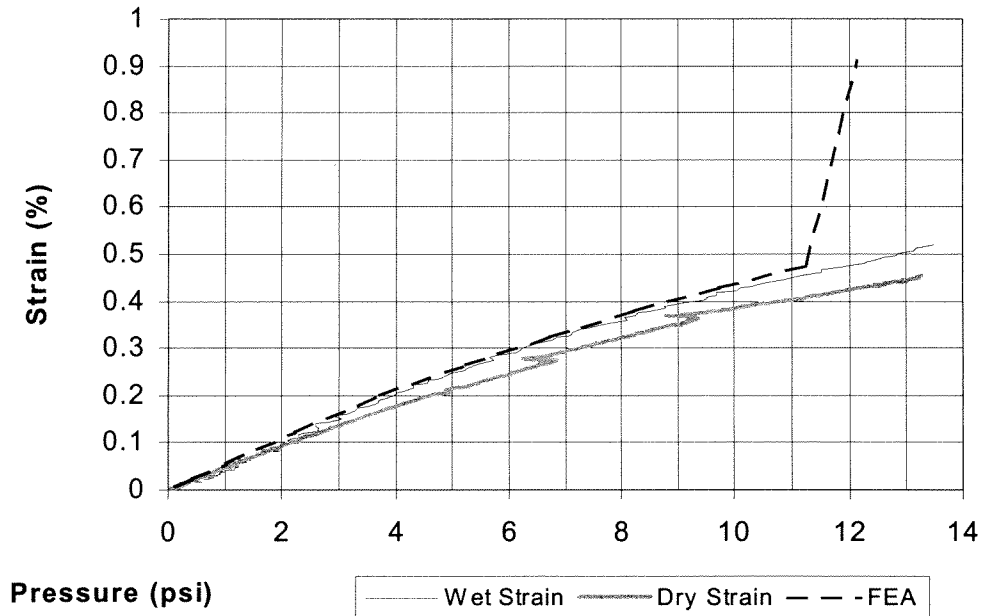


Fig. 11 Measured and predicted strains in J/24 hull panel

for the panel. As with the deflections, the correlation between this model and the wet and dry strain measurements was excellent. This illustrates the importance of boundary conditions in panel tests and in correlating measurements to FEA predictions.

The nonlinear analysis also included a progressive ply-failure routine, which is reflected in the jump in deflections near 11 psi on the nonlinear “frame and panel” curve in Fig. 11. As with the linear analysis, initial failure was predicted in Ply #7, a mat ply that was not the ply farthest from the neutral axis. The nonlinear analysis increased the failure limit by roughly 50%, illustrating the importance in design of using the appropriate analytical tools. As the actual panels did not fail at the point predicted by the nonlinear FEA, and due to the test machine’s limit of 15 psi, the error in the analysis is not known. As with flexural coupons the error is

likely caused by the too low strength values obtained from the tensile tests.

The panel studies illustrated a number of important elements in marine composites design. One was the effect of large deformations combined with selecting the proper finite element parameters and analysis models. The need for nonlinear responses from both strength and deflection criteria are not addressed by the linear beam and panel models used in many design codes and in practice. Additionally, the complex nature of coupled response caused by the typically unbalanced marine laminates negates the use of any “blended properties” structural methods. Finally, the combination of a low-strain-to-failure material such as chopped mat in an inner ply, when used with a higher strain material (cloth) as the outer ply, illustrates the potential case where the outer fibers are not the first to fail in bending.

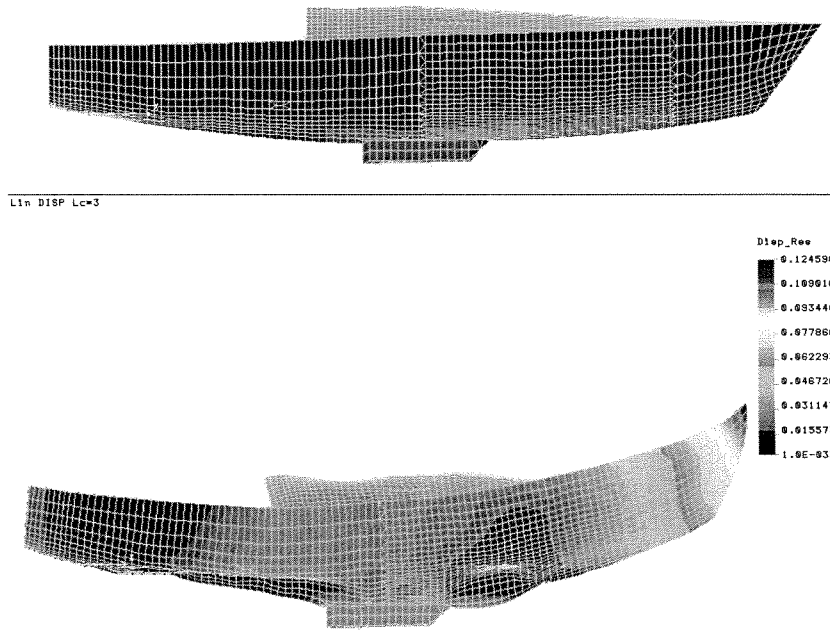


Fig. 12 Longitudinal deformations due to rig loads

Global model FEA

Full-scale results relied on a global model of the *J/24*. This was compared with results from the coupon and panel tests

and data from the on-the-water testing. The model represented an unfatigued vessel where the outer, submerged hull laminate had reached moisture equilibrium. The global *J/24* FEA model was developed using construction drawings and

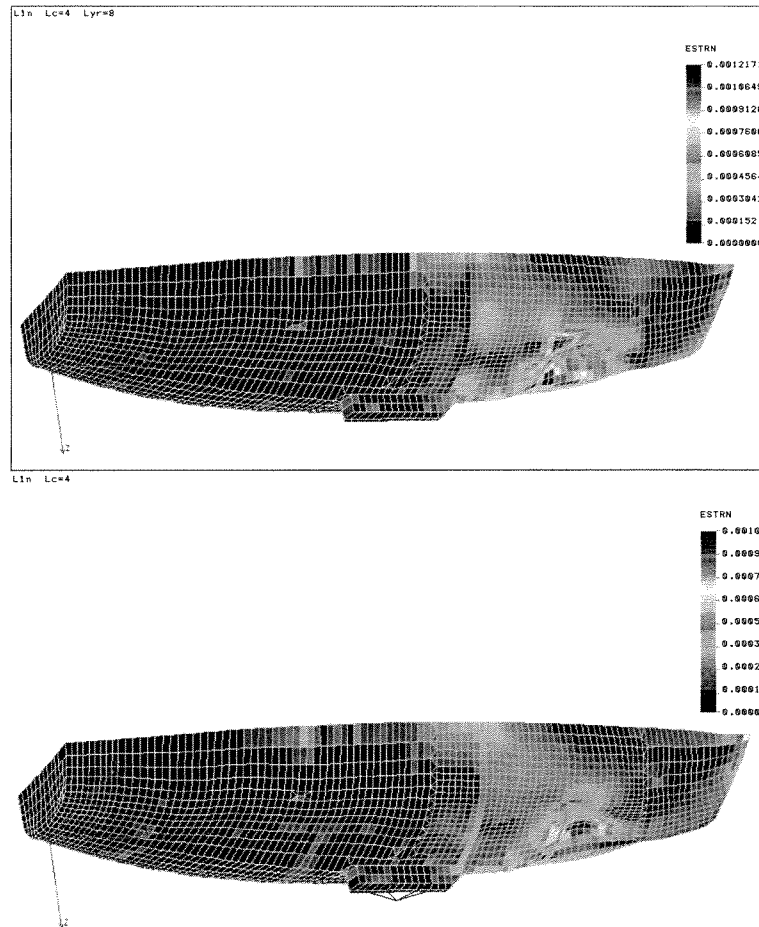


Fig. 13 Slamming strain plot for (top) inner (cloth) and (bottom) outer (mat) layers, $ws = 12.5$ knots, $H_S = 1$ ft

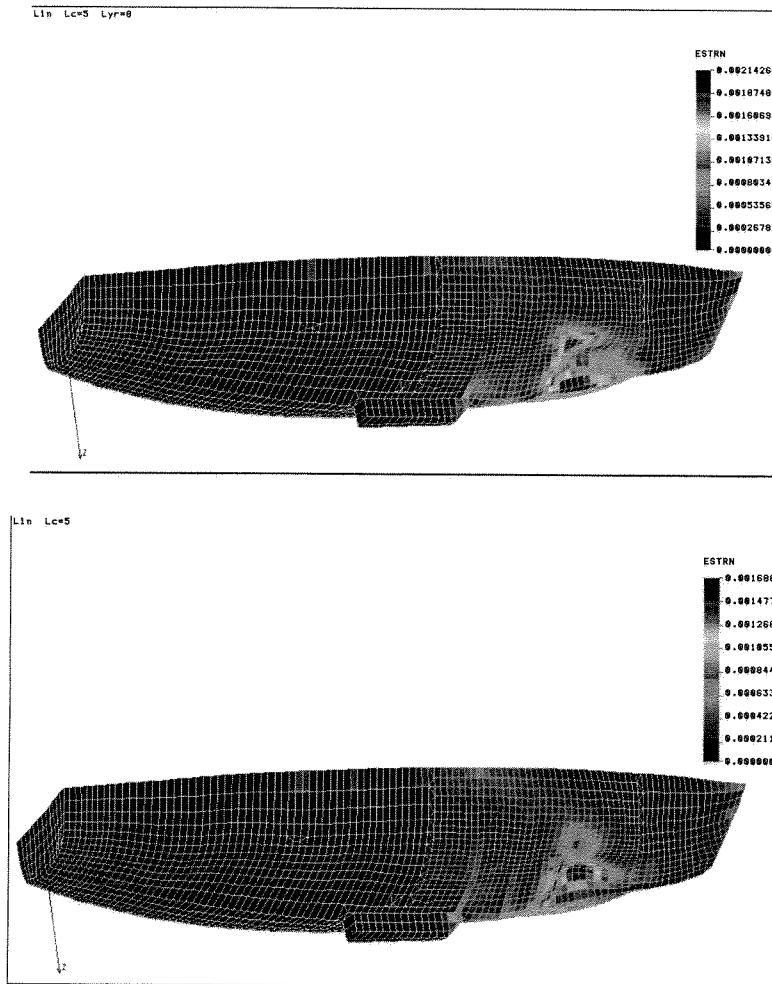


Fig. 14 Slamming strain plot for (top) inner (cloth) layer and (bottom) outer (mat) layer, $w_s = 22.5$ knots, $H_s = 2$ ft

data provided by TPI and boat checks performed at OCSC. All structural components were modeled and all weight items were included. The meshing for composite materials used laminated shell elements, with 95% quad elements and 4% triangular elements. The triangular elements were used to transition the mesh density. Isotropic materials used regular shell elements. Some rigid bar elements were used to connect a mass node simulating the center of gravity of the lead keel to the composite keel stump. Mass nodes were also used to represent other heavy, nonstructural components such as the rudder and outboard motor bracket. The mainsheet traveler and jib tracks were modeled using beam elements as detailed stresses were not needed for these components. The mesh density was increased in the slamming area. The model included 8424 elements.

Numerous model validation checks were made prior to the final sailing tests. The last check included a dockside test of each boat where rig loads were applied and strains and deflections were measured. The general approach used a tight string led between the bow and stern pulpits and alongside the mast. As the boat bent the string moved up the mast,

Table 8
Predicted and measured stiffness reduction for J6 and *Imagination*

	<i>Imagination</i>	J6
Predicted Stiff Reduction	-3%	-14%
Measured with Strain Gauges	-4%	-18%
Global "String Test"	-14%	-52%

providing an easy comparison to the FEA predictions. The simple string test correctly modeled the loss of stiffness trend, but over-predicted the amount significantly. As the string test included components not modeled by the FEA or measured by the strain gages, such as the mast and pulpits, the higher deflections are not surprising. For those wishing to determine if their vessel has lost stiffness, the simple string test, by amplifying the results to a level measurable by common tools, is a viable option.

Figure 12 shows the undeformed and deformed models. The lightly used boat was 14% less longitudinally stiff than predicted for an unfatigued boat and the heavily used boat was 52% less stiff.

The final FEA was to compare the vessels' predicted bending response in the wind and sea conditions seen during the on-the-water testing to measurements taken from the strain gages. Rig loads were based on an equilibrium analysis using the windward shroud and forestay strain gage readings as the primary inputs. Hydrostatic loading was based on wave elevation profiles scaled off photographs of the boats sailing. Hydrodynamic slamming loads used the Von Karmen pressure equation with the vertical acceleration components derived from the accelerometer data. The area subjected to slamming was based on analytical and experimental studies of sailing vessels [52,53] combined with photographs of the testing. With significant dynamic (transient) pressure loads the FEA analysis needed to match the vertical and rotational accelerations experienced by the vessel and eliminate excessive boundary condition reaction forces.

To generate the strains seen by the vessels in different wind and wave conditions the analysis was performed for wind speeds of 12.5, 17.5 and 22.5 knots. A second-order curve was fit through the strain predictions for intermediate winds.

Figure 13 shows the inner and outer layer strain plots resulting from the slamming. The 17% greater strain on the inner skin was due to the combination of the unbalanced laminate construction and the superposition of rig and wave loads.

The maximum predicted strain for the 12.5 knots of wind and 1 ft seas was 0.12%. As the failure strain is 0.93% for the dry condition and 0.90% for the wet condition this means that in moderate conditions the hull is routinely seeing strains equal to 13% of failure strain. As the flexural fatigue experiments presented previously showed, the endurance limit was between 12.5 and 25% of the failure strain; this means no significant fatigue would occur on J/24's sailing in wind speeds below 12 knots.

To model the maximum conditions routinely seen by the vessel, 22.5 knots and 2 ft seas, the vessel was heeled 25 deg and the freeboard forward was 6 in., corresponding to the bow nearly burying itself in a wave. Freeboard aft was greater, with the transom bottom submerged only 2 in. Again, these wave surface elevations were scaled off photos and the model was balanced for instantaneous equilibrium. Figure 14 shows plots similar to those presented for the 12.5-knot condition. In the stronger conditions the maximum strain was 0.214%, corresponding to 24% of failure strain. Based on the flexural fatigue coupon results, fatigue will occur.

To develop the stress response distribution, models were run for wind conditions ranging from 10 knots to 25 knots. Corresponding to the wave height distributions the stress distribution was grouped in 5 knot increments with the mean stress at the middle of the range (i.e., 12.5 knots, 17.5 knots, 22.5 knots). The maximum strains, as a percentage of failure, were 13%, 19% and 24%.

Cumulative damage correlation

The final step in determining and correlating the predicted stiffness reduction was to discretize and solve for the total stiffness reduction. Recalling that the total expected damage during T is:

$$E[D] = T \cdot f \int_0^\infty \frac{p(s_i) ds}{N(s_i)}$$

Replacing the continuous probability distributions with discretized distributions this becomes

$$T \cdot f = p(\phi) \cdot p(m) \cdot p(U_{ws}) \cdot \left[f(U_{ws}) + \frac{U(\phi, U_{ws}) \cdot \cos(\phi)}{U_w(U_{ws}) \cdot T_s(U_{ws})} \right]$$

where

- D = accumulated damage ratio (stiffness or strength)
- $p(\)$ = probability distribution function result for that component
- f = heading angle relative to upwind
- m = monthly usage
- U = boat speed (ws refers to wind speed)
- U_w = wave speed
- T_s = significant wave period (see Fig. 8-5)
- $n(s_{fi})$ = number of stress cycles at stress fi
- $N(s_{fi})$ = the number of cycles to failure at stress fi

The total damage accumulated is then:

$$D = \sum_{i=1}^j p(\phi)_i \cdot p(m)_i \cdot p(U_{ws})_i \cdot \left[f(U_{ws})_i + \frac{U(\phi, U_{ws})_i \cdot \cos(\phi)_i}{U_w(U_{ws})_i \cdot T_s(U_{ws})_i} \right] \frac{n(s_{fi})}{N(s_{fi})}$$

Table 8 compares the predicted and measured stiffness reductions for the slamming area hull laminate of *J6* and *Imajination* compared to an unfatigued vessel. For reference, the global, longitudinal stiffness string test data are also shown.

The correlation is reasonable given the potential variances in manufacturing between the coupons and the two vessels and the significance of low-cycle fatigue, where the vessels' histories are unknown. In the case of *J6*, if, as seen in the flexural coupon studies, a 25% reduction in stiffness signals near-term fatigue failure, then some hull laminate failures are likely in 4–7 years of use at the current rate.

Conclusions and recommendations

The objective of this study was to document, evaluate and improve the current methods of fatigue analysis for marine composites through a detailed analytical and experimental program. Specific conclusions were:

1. "Traditional" single-value reduction factors on composite material properties for fatigue effects are not appropriate in most situations. These can lead to unconservative designs. For example, using a cumulative FOS of four for these materials would be risky as the coupon tests showed that stiffness loss over time was evident at this stress level.
2. Four-point bend tests yield acceptable results if the laminate is designed for tensile face failure and the span is large enough that core shear failure is unlikely.
3. Effects of long-term moisture exposure cannot be reliably predicted through boil tests. In this case the boil test led to significant conservatism. For laminates with low fiber volumes tensile properties as well as shear and compressive properties are effected. Significant differences were seen in the number of flexural cycles to failure, even though the inside surface, which failed first, was dry in both cases.
4. Panel testing can, in some cases, be replicated by finite-element analysis and coupon tests. In cases where FEA is planned due to the complexity of structure, panel tests may not be needed. In other cases, either FEA or panel tests can be used, although FEA offers significantly greater flexibility at the cost of operator training.
5. Relatively dense meshes are required to accurately model stresses and panel deflections when using linear shell elements. For high-cycle fatigue applications this is acceptable as in-plane deflections remain in the linear range of composites. Low-cycle applications should use a nonlinear modulus profile to accurately model deflections and stresses.
6. Linear shell elements can provide accurate results for out-of-plane loading, and can be improved by applying a single-step, in-plane, added-stiffness approximation. In cases where large deformation is combined with multi-axis loading, such as boundary constraints, geometric nonlinear analysis is required.
7. Edge-sealing did not influence moisture absorption rates of these uncured polyester laminates. Varnishing the edges of balsa-cored laminates prevents moisture absorption into the core while not significantly affecting stiffness.
8. The common marine practice of having thicker outer

skin laminates can be justified for more than just abrasion resistance. With reduced strength due to compression and moisture effects, and for practical reasons of water integrity, the common practice leads to first failure occurring with tensile failure of the inner skin. Similarly, moisture absorption by the outer hull-skin did not significantly affect panel bending or strength, although it did affect the number of fatigue cycles to failure.

9. A simple, visual clue as to the onset of rapidly increasing fatigue failure is the onset of "whitening" of the resin. The size of the initial failure spots corresponds to the weave crimp dimensions. This could be used by surveyors to identify fatigue failure onset.
10. Stiffness reduction due to fatigue can be significant on small craft made of composites. In the case of some highly-stressed boats this verifies a commonly held opinion of boats going "soft." Design load reduction factors of 4–8 are needed with polyester/E-glass (mat/cloth) laminates to avoid service-life stiffness reduction.
11. Polyester resins, which have failure strains of approximately 1% are not well matched to E-glass, which has a failure strain of nearly 5%. This leads to microcracking at a small portion of the fibers' ultimate strength, resulting in large moisture absorption and stiffness loss. Better combinations would include epoxy and vinyl ester resins that have failure strains of 4–7%.
12. Standard methods used for fatigue analysis of metal vessels can be applied to composite vessels, but unique S-N curves must be developed for each laminate.
13. A "Miner's-type" damage accumulation approach can also be applied to stiffness reduction. Like the strength reduction, stiffness reduction in marine composites is dominated by large amplitude, low-cycle events. A few "significant events," such as collisions, can cause the same amount of stiffness reduction as thousands of waves.
14. A relatively simple "string" test can be used to check a vessel's static stiffness. This also gives a good indication of the dynamic global bending stiffness. The string test may overpredict the loss of stiffness, however, as it also includes the mast and pulpits and their connections to the hull and localized stress risers such as the laminate below the mast step and the stem fitting.
15. The "service-life" of recreational craft is difficult to predict. Designers should realize that some vessels may experience 10^7 significant wave loading cycles. As most composite fatigue data only carries to 10^6 cycles this requires a higher safety margin.

Although this project necessarily looked at a laminate that was commonly used 15 years ago, current technology has relegated the J/24 materials to low-cost marine applications. Follow-up studies should look at generating S-N curves for currently used laminates. These would include laminates using woven roving, boat cloth, unidirectionals, epoxy, and vinyl ester resins, honeycomb and foam cores, and fabrication methods such as vacuum-bagging, SCRIMP, and pre-pregs. In particular, epoxy and vinyl ester resins should be explored as they appear to have greater fatigue tolerance.

Acknowledgments

The author would like to thank the numerous people who helped during the project's six-year duration and, in particular, Professors Bob Bea, Hari Dharan and Alaa Mansour of the University of California at Berkeley and Mr. Steve Slaughter of MCA Engineers for guidance. The American Bu-

reau of Shipping, TPI, OCSC, Maricomp and the United States Naval Academy Research Council (through the Office of Naval Research, grant N0001499WR20020) provided much appreciated financial, material and software support.

References

1. Davis, G. T., "In Service Failures from the Marine Surveyor Point of View," in *4th International Conference on Marine Applications of Composite Materials*, 1992, Melbourne, Florida, Composites Education Assoc.
2. Forbes, H., Laing, M., and Myatt, J., *Fastnet Race Inquiry*, 1979, Royal Yachting Assoc. Royal Ocean Racing Club.
3. Smith, L. E., "Technical Issues and Design Challenges of Composite Marine Structures," in *Application of Composites to the Marine Environment*, 1993, Savannah, Georgia.
4. Martinsen, S. and Madsen C., "Production, Research and Development in GRP Materials at Danyard Aalborg A/S," in *3rd International Conference on Marine Applications of Composite Materials*, 1990, Florida Institute of Technology.
5. Hashin, Z., "Analysis of Composite Materials—A Survey," *Journal of Applied Mechanics* Vol. 50 (September), 1983, pp. 481–505.
6. Lubin, G., *Handbook of Composites*, 1982, Van Nostrand Reinhold Company.
7. Tsai, S., *Composites Design*, 4th ed., 1988, Dayton, Ohio, Think Composites.
8. Smith, C. S., *Design of Marine Structures in Composite Materials*, 1990, Barking Essex, England, Elsevier Science Publishers.
9. FPL, *Forest Products Laboratory: The Encyclopedia of Wood: Revised Edition*, 1989, New York, Sterling Publishing.
10. Summers, C., "Building the 161' FRP Yacht *Evviva*," *Professional Boatbuilder*, 1994, pp. 18–21.
11. Hepburn, R. D., Magliulo, G., and Wright, T., "The U.S. Navy's New Coastal Minehunter (MHC): Design, Material, and Construction Facilities," *Naval Engineers Journal*, 1991, May.
12. "GRP Minehunter Launched," in *Workboat*, 1994, p. 180.
13. NRC, *Use of Composite Materials in Load-Bearing Marine Structures*, Vol. 1, 1990, National Research Council.
14. NRC, *Use of Composite Materials in Load-Bearing Marine Structures*, Vol. 2, 1990, National Research Council.
15. Helme, S., *North American Sailing Industry Study*, 1993, International Marine.
16. Anon., "Shipyard Contracts," in *Marine Log*, 1994.
17. Anon., "Title XI Catapults U.S. Yards into the Export Market," in *Marine Log*, 1994.
18. NMMA, *Boating 1993*, 1994, National Marine Manufacturers Association.
19. Greene, E., *Marine Composites*, 1990, Ship Structures Committee.
20. Bea, R. G., *Reliability Based Design Criteria for Coastal and Ocean Structures*, 1990, Barton, Australia, The Institution of Engineers, Australia, 221.
21. ABS, *Rules for Building and Classing Reinforced Plastic Vessels*, 1978, American Bureau of Shipping.
22. ABS, *Guide for Building and Classing Offshore Racing Yachts*, 1986, American Bureau of Shipping.
23. ABS, *Guide for Building and Classing High Speed Craft*, 1997, American Bureau of Shipping.
24. Warren, Q., "A Builder's Designer," in *Professional Boatbuilder*, 1999, pp. 66–80.
25. Gibbs & Cox, I., *Marine Design Manual for Fiberglass Reinforced Plastic*, 1960, New York, McGraw-Hill Book Co.
26. Spaulding, K. B., Jr., "Fiberglass Boats in Naval Service," *Naval Engineers Journal*, 1966, April.
27. Sheno, R. A. and Wellicome, J. F., Eds., *Composite Materials in Maritime Structures*, Cambridge Materials in Maritime Structures, Cambridge Ocean Technology Series, 1993, Cambridge.
28. Jakubowski, J. C., "Stiffness Reduction of Marine Laminates Due to Constant Amplitude Deflection Fatigue Loading," in *International Conference on Marine Applications of Composite Materials*, 1990, Melbourne, Florida, Composites Education Association.
29. Tsai, S. W. and Hahn, H. T., *Introduction to Composite Materials*, 1980, Lancaster, Pennsylvania, Technomic, 453.
30. Hashin, Z., "Failure Criteria for Unidirectional Fiber Composites," *ASME Journal of Applied Mechanics*, Vol. 47, 1980, pp. 329–334.
31. Hughes, O. F., *Ship Structural Design*, 1988, Jersey City, New Jersey, The Society of Naval Architects and Marine Engineers.
32. Loveless, H. S., Ingle, L. R., and Gerrard, C. E., "Fatigue and Its Relationship to End-Use Performance," *Physical Testing of Plastics—Correlation with End-Use Performance*, ASTM STP 736, 1981.
33. Mull, G. W., "Small Craft Structures for the Eighties and Beyond (draft)," in *The New England Sailing Yacht Symposium*, 1988, Mystic, Connecticut.
34. Hofer, K. E., Stander, M., and Bennet, L. C., "Degradation and Enhancement of the Fatigue Behavior of Glass/Graphite/Epoxy Hybrid

Composites After Accelerated Aging," in *SPI Annual Conference*, 1977, Washington, DC, Reinforced Plastics/Composites Institute.

35. Collins, J. A., *Failure of Materials in Mechanical Design*, 2nd ed., 1993, New York, John Wiley & Sons, p. 654.

36. Schaff, J. R. and Davidson, B. D., "Life Prediction for Composite Laminates Subjected to Spectrum Fatigue Loading," in *Durability of Composite Materials*, 1994, ASME, pp. 89-109.

37. ASTM, *ASTM Standards and Literature References for Composite Materials*, 1978, American Society for Testing and Materials.

38. Burke, S., Fax of July 29, 1998.

39. WindCall, *Wind Reports*, 1999, Call of the Wind, Inc.

40. Chou, S. J., *Ship Motions and Capsizing in Astern Seas*, 1974, University of California at Berkeley.

41. Sorensen, R. M., *Basic Wave Mechanics for Coastal and Ocean Engineers*, 1993, New York, John Wiley & Sons.

42. Pond, S. and Pickard, G. L., *Introductory Dynamical Oceanography*, 2nd ed., 1983, Oxford, U.K., Pergamon.

43. Army, U., *Shore Protection Manual*, 4th ed., Vol. 1, 1984, Vicksburg, Mississippi, U.S. Army Corps of Engineers.

44. IMS, *IMS Velocity Prediction Program Speed Predictions for J/24 Class Sailboat*, 1996, U.S. Sailing, Portsmouth, Rhode Island.

45. Springer, G., Ed., *Environmental Effects on Composite Materials*, 1981, Technomic, Westport, Connecticut.

46. Sloan, F. E., *The Effects of Long-Term Seawater Exposure on Graphite/Epoxy Composite Materials*, 1991, University of California at San Diego.

47. Bea, R. G., *The Role of Human Error in Design, Construction, and Reliability of Marine Structures*, 1994, Ship Structures Committee: Washington, DC.

48. Scott, R. J., *Fiberglass Boat Design and Construction*, 1996, Jersey City, New Jersey, The Society of Naval Architects and Marine Engineers.

49. Cook, R., Malkus, D., and Plesha, M., *Concepts and Applications of Finite Element Analysis*, 3rd ed., 1989, John Wiley & Sons.

50. Mindlin, R. D., "Influence of Rotary Inertia and Shear on Flexural Motion of Isotropic Elastic Plates," *Journal of Applied Mechanics*, Vol. 18, 1952, pp. 31-38.

51. DiSciuva, M., "An Improved Shear-Deformation Theory for Moderately Thick Multilayered Anisotropic Shells and Plates," *ASME Journal of Applied Mechanics*, Vol. 54, 1987, pp. 589-596.

52. Riber, H. J., *Strength Analysis of the 470 Sailing Boat*, 1993, Technical University of Denmark, Lyngby.

53. Hamilton, J. and Patterson, J., "America's Cup Yacht Structural Design: Finite Element Analysis and Laminate Optimization," in *SAMPE*, 1992, Anaheim, California, Society for the Advancement of Materials Processing and Engineering.